AIAA 99-3523

Unsteady Flows in Semi-Infinite Expanding Channels with Wall Injection

E. C. Dauenhauer and J. Majdalani
Marquette University
Milwaukee, WI 53233

30th AIAA Fluid Dynamics Conference
28 June–1 July 1999
Norfolk, VA

Unsteady Flows in Semi-Infinite Expanding Channels with Wall Injection

E. C. Dauenhauer* and J. Majdalani†
Marquette University, Milwaukee, WI 53233

The current article presents an exact similarity solution of the Navier-Stokes equations for unsteady flows established in a semi-infinite rectangular channel. The case considered here pertains to a channel that experiences injection through two opposing porous walls while undergoing uniform expansion. In the analysis, the Stokes' stream function and the vorticity equation are used in concert to yield an ordinary differential equation that lends itself to a similarity solution in space and time. Following this similarity transformation, the original problem is reduced to solving a single fourth-order differential equation with four boundary conditions. The mathematical procedure is somewhat reminiscent of the classic Berman approach. It is found that, in rectangular chambers and ducts where wall regression and injection occur simultaneously, the streamlines, pressure distributions, and shear stresses are time and space dependent. They can be characterized by two dimensionless parameters: the expansion ratio of the walls α and the cross-flow Reynolds number *R*. Instances of direct application include the modeling of pulsating diaphragms with permeable walls and the grain regression during solid rocket motor combustion. In order to examine the incompressible laminar flow character in the channel, a numerical scheme is devised. The scheme is based on a shooting method that can be applied in conjunction with a fourth-order Runge-Kutta technique. The algorithm requires solving a set of twelve first-order differential equations with two unspecified start-up conditions. In seeking the two unknown initial guesses, the inverse Jacobian method is used to accelerate the convergence process.

I. Introduction

THE current paper presents a procedure that leads to an exact similarity solution of the Navier-Stokes equation in semi-infinite rectangular channels with porous and uniformly expanding walls. The solution to be developed provides the means to fully characterize the flow field established in such a physical setting. One of the objectives will be, therefore, to extend our current knowledge of flow analyses involving channels with porous walls.

Laminar flow studies in permeable walls have received considerable attention in the past due to their relevance to a number of engineering applications. These include binary gas diffusion, filtration, ablation cooling, surface sublimation, grain regression (as in the case of combustion in solid rocket motors), and the modeling of air and blood circulation in the respiratory system.

The earliest studies of steady flows through permeable and stationary walls can be traced back to Berman[1] who investigated the laminar, two-dimensional flow of a viscous incompressible fluid driven by uniform injection (or suction) in a rectangular channel with porous walls. In his study, Berman assumed that the transverse velocity component was independent of the streamwise coordinate. He thus reduced the Navier-Stokes equations to a single, nonlinear, fourth-order, ordinary differential equation (ODE) with four boundary conditions and a cross-flow Reynolds number R. The latter was based on the normal injection speed v_w and channel half-spacing h. For small R, he employed a regular perturbation scheme to derive an asymptotic formulation. Numerous studies of channel flows with permeable walls followed. These included the works of Sellars,[2] Terrill[3] (who extended Berman's small R case), Proudman[4] (who investigated the large R case using an integral approach), Morduchow[5] (who applied the method of averages over the entire injection range), White *et al.*[6] (who provided for an arbitrary R a convergent power series solution), Taylor,[7] and Yuan[8] (who provided analytic solutions for the infinite and large injection cases, respectively). Improvements to the latter were provided by Terrill.[9]

*Student Member AIAA.
†Assistant Professor, Department of Mechanical and Industrial Engineering. Member AIAA.

For unsymmetrical flows caused by different wall velocities, Terrill & Shrestha[10] constructed a generalized perturbation series for small R. For large injection, Shrestha & Terrill[11] extended Proudman's one-term expression using matched asymptotic expansions. In the same vein, Cox[12] considered the practical case of an impermeable wall opposing a transpiring wall.

Treatments of moving boundaries can be attributed to Brady & Acrivos[13] who presented an exact solution to the Navier-Stokes equations for a flow driven by an axially accelerating surface velocity and symmetric boundary conditions. Their work was motivated by the need to study long slender droplets trapped in extensional flows. This was later generalized by Watson *et al.*[14] who allowed the accelerating walls to be permeable. Watson[15] also examined the case of asymmetrically accelerating walls.

In validating the similarity solutions recounted above, investigators have constantly relied on numerical simulations. Experimental verifications have also been accomplished. In fact, numerous laboratory experiments on steady channel flow through porous walls have been conducted by Taylor,[7] Varapaev & Yagodkin,[16] Raithby & Knudsen,[17] and Sviridenkov & Yagodkin.[18]

The addition of time-dependent motion in a long rectangular channel with porous walls was achieved experimentally by Ma *et al.*[19,20] and Barron *et al.*[21] In fact, both used the sublimation process of carbon dioxide to simulate the injection process at the walls. As a result, the walls of their channel expanded during the sublimation process. Other physical settings that are better modeled with expanding permeable walls include the regression of the burning surface in solid rocket motors and the pulsation of porous diaphragms. For instance, in simulating the laminar flow field in cylindrical solid rocket motors, Goto and Uchida[22] have analyzed the laminar incompressible flow in a semi-infinite porous pipe whose radius varied with time. The present analysis extends their analysis to expanding channels and ducts which are rectangular in constitution and possess porous and transpiring walls.

II. Formulation

We consider a rectangular channel of semi-infinite length which possesses a high aspect ratio of width to height. In actuality, the channel is of finite length, however, it is commonplace in the literature to assume semi-infinite length in order to neglect the influence of the opening at the end.[23] The other end is closed by a solid membrane which is allowed to stretch with channel expansion. The axial flow is zero at the closed end $(x = 0)$ due to the fluid's viscosity and thus, the closed end can be employed as a symmetry plane. This

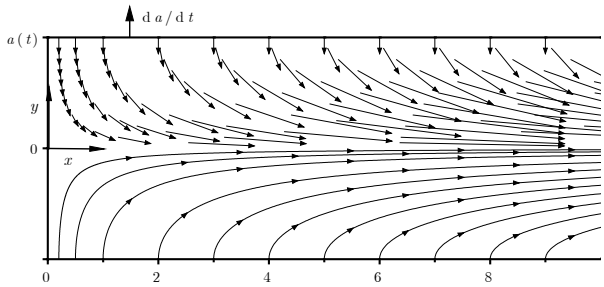

Fig. 1. Coordinate system and bulk fluid motion.

is illustrated in Fig. 1. With x indicating the axial direction and y the transverse direction, the corresponding axial and transverse velocity components are defined as u and v, respectively. With this notation, the fundamental equations governing the unsteady flow of an incompressible fluid are the classic continuity and momentum expressions:

$$\frac{\partial u}{\partial x} + \frac{\partial v}{\partial y} = 0 \tag{1}$$

$$\frac{\partial u}{\partial t} + u\frac{\partial u}{\partial x} + v\frac{\partial u}{\partial y} = -\frac{\partial p}{\partial x}\cdot\frac{1}{\rho} + \nu\left(\frac{\partial^2 u}{\partial x^2} + \frac{\partial^2 u}{\partial y^2}\right) \tag{2}$$

$$\frac{\partial v}{\partial t} + u\frac{\partial v}{\partial x} + v\frac{\partial v}{\partial y} = -\frac{\partial p}{\partial y}\cdot\frac{1}{\rho} + \nu\left(\frac{\partial^2 v}{\partial x^2} + \frac{\partial^2 v}{\partial y^2}\right). \tag{3}$$

where ρ, p, ν, and t are the density, pressure, kinematic viscosity, and time. The channel walls of interest regress only in the transverse direction and their separation is a function of time only. Under the porous wall stipulation, the fluid is injected or extorted uniformly and orthogonally through the channel walls at a velocity v_w. The latter is proportional to the expanding wall surface velocity. The boundary conditions necessary for solving the continuity and momentum equations are:

$$u = 0 \qquad v = v_w = -A\dot{a}\,;\, y = a(t) \tag{4}$$

$$\frac{\partial u}{\partial y} = 0 \qquad v = 0\,;\; y = 0 \tag{5}$$

$$u = 0\,;\; x = 0\,. \tag{6}$$

The injection coefficient A is a measure of the porosity of the wall and can be utilized as a control parameter in the final solution.

By applying mass conservation to a volume of fluid extending from $x = 0$ to x, the mean flow velocity $u_m(x)$ can be found to be proportional to x:

$$u_m = -\frac{\dot{a}x}{a}\,. \tag{7}$$

At this point, the Stokes stream function can be introduced. This allows replacing the two velocity components by one single function

$$u = \frac{\partial \psi}{\partial y}, \text{ and } v = -\frac{\partial \psi}{\partial x}. \tag{8}$$

By definition of the stream function, the continuity equation is automatically satisfied and thus no longer useful in determining ψ.

A new variable can now be removed at the expense of introducing another. In fact, the vorticity transport equation for the given geometry can be arrived at by taking the curl of the momentum equation. This operation eliminates the pressure from the momentum equation and introduces, in its stead, the flow vorticity. This is illustrated below. Starting with

$$\nabla \times \left(\frac{D\vec{V}}{Dt} = -\frac{1}{\rho} \cdot \nabla p + \nu \nabla^2 \vec{V} \right) \tag{9}$$

gives $$\frac{\partial \zeta}{\partial t} + u\frac{\partial \zeta}{\partial x} + v\frac{\partial \zeta}{\partial y} = \nu \left(\frac{\partial^2 \zeta}{\partial x^2} + \frac{\partial^2 \zeta}{\partial y^2} \right) \tag{10}$$

where $$\zeta = \frac{\partial v}{\partial x} - \frac{\partial u}{\partial y}. \tag{11}$$

III. Mathematical Procedure

A. Similar Solution in Space

A similar solution with respect to x can be developed due to mass conservation, since the variation of the channel height is uniform along the axial direction. Following Berman's classic approach, and in view of the boundary conditions represented by Eqs. (4) -(5), a similar solution can be assumed to be of the form

$$\psi = \nu x f(a) F(\eta, t), \text{ where } \quad \eta = \frac{y}{a} \tag{12}$$

and $F(\eta,t)$ is independent of the axial coordinate. Placing Eq. (12) into Eq. (8), the axial and transverse velocities can be expressed as a function of F:

$$u = \frac{\nu x}{a} f(a) F_\eta, \text{ and } \quad v = -\nu f(a) F(\eta, t) \tag{13}$$

where $F_\eta = \partial F / \partial \eta$. At this point, we notice that $u_{xx} = v_x = 0$. The association $f(a) = 1/a$ can then be determined when $u_{xx} = v_x = 0$ is inserted into the vorticity equation and the dimensions of the inertial and viscous terms are compared. With this realization, the axial and transverse velocities can be written in their final form, namely,

$$u = \frac{\nu x}{a^2} F_\eta, \quad \text{and} \quad v = -\frac{\nu}{a} F(\eta, t). \tag{14}$$

Noting that the transverse velocity v is independent of x, the vorticity equation simply reads

$$\zeta = -\frac{\partial u}{\partial y} \tag{15}$$

and Eq. (3) will then be $p_{yx} = 0$. Upon substitution of Eq. (15) and Eq. (1) into the vorticity transport expression given by Eq. (10), one obtains

$$u_{yt} + u u_{yx} + v u_{yy} = \nu u_{yyy}. \tag{16}$$

By inserting the velocity expression from Eq. (14) into Eq. (16), we can develop a differential equation for our function F. The result is

$$\left[F_{\eta\eta\eta} + F F_{\eta\eta} + F_\eta \left(2\alpha - F_\eta \right) + \alpha \eta F_{\eta\eta} - \frac{a^2}{\nu} F_{\eta t} \right]_\eta = 0 \tag{17}$$

where α is the Wall Expansion Ratio defined as

$$\alpha(t) = \frac{\dot{a} a}{\nu}. \tag{18}$$

Allowing $p_{xy} = 0$ in Eq. (2), this will also lend itself as a method of arriving at Eq. (17). The boundary conditions given by Eq. (4)-(5) should then be updated to account for the normalization:

$$\begin{array}{lll} F_{\eta\eta} = 0, & F = 0; & \eta = 0, \\ F_\eta = 0, & F = A\alpha = R; & \eta = 1. \end{array} \tag{19}$$

By equating the expression we had before in Eq. (4), $v = -A\dot{a}$, with the expression for the transverse velocity in Eq. (14) and inserting the expansion ratio α where applicable, we recognize that our function F is a product of the injection coefficient A and the expansion ratio α. Since this occurs at the permeable wall, we can write $R = A\alpha = -a v_w / \nu$ where R is the cross-flow Reynolds number.

B. Similar Solution in Space and Time

A similar solution with respect to space and time can now be developed. If our function F is assumed to be dependent on η only and that α is constant, it follows

that $F_{\eta t} = 0$. The value of the expansion ratio α can be specified by its initial value

$$\alpha = \frac{\dot{a}a}{\nu} = \frac{\dot{a}_o a_o}{\nu} \tag{20}$$

with a_o and $\dot{a}_o = da_o / dt$ denoting the initial channel height and channel expansion ratio, respectively. By integrating Eq. (20) with respect to time, a similar solution for the channel height variation with time can be obtained. This is given by

$$\frac{a}{a_o} = \left(1 + \frac{2\nu\alpha t}{a_o^2}\right)^{\frac{1}{2}}. \tag{21}$$

Subsequently, an expression for the injection velocity variation can be deduced provided that the injection coefficient A in Eq. (4) is held constant:

$$\frac{\dot{a}}{\dot{a}_o} = \frac{v_w}{(v_w)_{t=0}} = \left(1 + \frac{2\nu\alpha t}{a_o^2}\right)^{-\frac{1}{2}}. \tag{22}$$

Now, an ODE for the function F can be realized by direct integration of Eq. (17)

$$F''' + FF'' + F'(2\alpha - F') + \alpha\eta F'' = K \tag{23}$$

where a prime replaces $d / d\eta$ and K is the constant of integration. The necessary boundary conditions translate into:

$$\begin{aligned} &F'' = 0, && F = 0; && \eta = 0, \\ &F' = 0, && F = A\alpha = R; && \eta = 1\ . \end{aligned} \tag{24}$$

C. Numerical Solution

Since we have four boundary conditions in Eq. (24) that are imposed on Eq. (23), it is convenient to eliminate the integration constant K by differentiating Eq. (23) with respect to η. The resulting governing ODE becomes:

$$F^{IV} + FF''' + F''(3\alpha - F') + \alpha\eta F''' = 0\,. \tag{25}$$

This can be solved numerically by applying a shooting method coupled with fourth order Runge-Kutta integration. The procedure adopted in resolving the function $F(\eta)$ is described next.

1. Shooting Method

The boundary conditions for Eq. (25) can be redefined as

$$\begin{aligned} &F''(0) = 0, && F(0) = 0, \\ &F'''(0) = k, && F'(0) = t \\ &F'(1) = 0, && F(1) = A\alpha = R \end{aligned} \tag{26}$$

where t and k are initial guesses introduced as dummy variables and t should not be confused with time. We can now express Eq. (25) in the following fashion:

$$\begin{aligned} y^{IV} &= f(x, y, y', y'', y''') \\ &= y''(y' - 3\alpha) - yy''' - \alpha x y''' \end{aligned} \tag{27}$$

where y should not be confused with the transverse location. Thus,

$$f = y''(y' - 3\alpha) - yy''' - \alpha x y'''\,. \tag{28}$$

The boundary conditions become

$$\begin{aligned} &y'''(0) = k, && y''(0) = 0, \\ &y'(0) = t, && y(0) = 0. \end{aligned} \tag{29}$$

To satisfy the boundary conditions at $\eta = 1$, the functions $g(t,k)$ and $h(t,k)$ are introduced such that

$$\begin{aligned} g(t,k) &= y(1,t,k) - R = 0 \\ h(t,k) &= y'(1,t,k) - 0 = 0\ . \end{aligned} \tag{30}$$

Based on Newton's Method, an algorithm for calculating the zeros t^* and k^* of Eq. (30) can be developed. The algorithm requires updating initial guesses following

$$\begin{bmatrix} t \\ k \end{bmatrix}_{n+1} = \begin{bmatrix} t \\ k \end{bmatrix}_n - [J]^{-1} \cdot \begin{bmatrix} y(1,t,k) - R \\ y'(1,t,k) \end{bmatrix}_n \tag{31}$$

where n is the iteration index and $[J]^{-1}$ is the inverse of the Jacobian matrix.

At this point, we introduce functions Z and W according to

$$Z(x,t,k) \equiv \frac{\partial y}{\partial t}, \text{ and } W(x,t,k) \equiv \frac{\partial y}{\partial k}. \tag{32}$$

Following this transformation, the boundary conditions can be expressed as illustrated in the following example for $Z_x(0,t,k)$

$$Z_x = \frac{\partial}{\partial x}\left(\frac{\partial y}{\partial t}\right) = \frac{\partial}{\partial t}\left(\frac{\partial y}{\partial x}\right) ,$$

then,

$$Z_x(0,t,k) = \frac{\partial}{\partial t}\left[y'(0)\right] = \frac{\partial}{\partial t}[t] = 1 . \qquad (33)$$

Likewise, the boundary conditions for Z and W in Eq. (28) become

$$\begin{aligned} Z(0,t,k) &= 0 & W(0,t,k) &= 0 \\ Z_x(0,t,k) &= 1 & W_x(0,t,k) &= 0 \\ Z_{xx}(0,t,k) &= 0 & W_{xx}(0,t,k) &= 0 \\ Z_{xxx}(0,t,k) &= 0 & W_{xxx}(0,t,k) &= 0 . \end{aligned} \qquad (34)$$

Next, the order of differentiation in Eq. (27) can be switched such as

$$\frac{\partial f}{\partial t} = \frac{\partial(y_{xxxx})}{\partial t} = \frac{\partial^4}{\partial x^4}\left(\frac{\partial y}{\partial t}\right),$$

Since $Z = \partial y / \partial t$, a fourth-order differential equation for Z can be generated in the form

$$Z^{IV} = f_y Z + f_{y'} Z' + f_{y''} Z'' + f_{y'''} Z''' \qquad (35)$$

whose boundary conditions are given in Eq. (34). Similarly, an expression involving W is found to be

$$W^{IV} = f_y W + f_{y'} W' + f_{y''} W'' + f_{y'''} W''' \qquad (36)$$

with the boundary conditions listed in Eq. (34).

Returning to Newton's Method that solves for the correct initial guesses, the Jacobian matrix is defined by

$$J = \begin{bmatrix} \frac{\partial f_1}{\partial t} & \frac{\partial f_1}{\partial k} \\ \frac{\partial f_2}{\partial t} & \frac{\partial f_2}{\partial k} \end{bmatrix} \quad ; \quad \begin{aligned} f_1 &= y - R \\ f_2 &= y' \end{aligned} , \qquad (37)$$

which simplifies to:

$$J = \begin{bmatrix} Z(1) & W(1) \\ Z_x(1) & W_x(1) \end{bmatrix}. \qquad (38)$$

Once the inverse of the Jacobian in Eq. (38) is determined, Eq. (31) reduces to

$$\begin{bmatrix} t \\ k \end{bmatrix}_{n+1} = \begin{bmatrix} t \\ k \end{bmatrix}_n - c \cdot \begin{bmatrix} W_x & -W \\ -Z_x & Z \end{bmatrix} \begin{bmatrix} y - R \\ y' \end{bmatrix}_n . \qquad (39)$$

Where $c = 1/\det(J) = [Z(1)W_x(1) - W(1)Z_x(1)]^{-1}$.

2. Runge-Kutta Solution Composition

The shooting method described above was chosen for its ease of conversion into a Runge-Kutta solution set. Twelve variables are chosen to represent y, Z, W, and their respective derivatives out to the third order. Differentiating each of these functions and performing the appropriate substitutions provides the solution set. The Runge-Kutta method is an effective approach in this application since it permits us to enter the prescribed boundary conditions only once for all twelve variables. Of course, our solution requires the input of initial guesses for the boundary condition values of t and k which are then iterated according to

$$\begin{aligned} t_{n+1} &= t_n + \frac{W(1)y'(1) + W_x(1)\left[R - y(1)\right]}{Z(1)W_x(1) - W(1)Z_x(1)} \\ k_{n+1} &= k_n + \frac{Z_x(1)\left[y(1) - R\right] - Z(1)y'(1)}{Z(1)W_x(1) - W(1)Z_x(1)} \end{aligned} . \qquad (40)$$

IV. Flow-Field Characterization

A. Non-dimensional Parameters

Once we obtain a numerical solution for the function $F(\eta)$, the dimensionless stream function and axial and transverse velocities will be available. The stream function can be normalized at $\eta = 1$ (at the wall) by considering Eq. (24), which then suggests letting $\psi_w = \nu x F(1)/a = \nu x R/a$. Consequently,

$$\frac{\psi}{\psi_w} = \frac{F}{R}. \qquad (41)$$

Additionally, the mean axial velocity in Eq. (7) becomes

$$\frac{u}{u_m} = \frac{F'}{R} \qquad (42)$$

for any axial position. Finally, the velocity at the wall, which is expressed as $v_w = -A\dot{a} = -\nu R/a$, becomes

$$\frac{v}{v_w} = \frac{\psi}{\psi_w} = \frac{F}{R}. \tag{43}$$

The normalized stream function and velocity components are shown in Figs. 2 and 3.

B. Pressure and Shear Distributions

To complete our flow-field analysis, the resulting pressure gradients and shear stress distributions are considered. An expression for the transverse pressure gradient can be developed by substituting the velocity components of Eq. (14) into Eq. (3) with F acting as a function of η only. The result is

$$p_\eta = -\nu^2 \rho a^{-2} \left[F_{\eta\eta} + F F_\eta + \alpha \left(F + \eta F_\eta \right) \right]. \tag{44}$$

The transverse pressure distribution is found by manipulating Eq. (44) before integration and application of the boundary conditions of Eq. (24). Proceeding by writing

$$\int_{p_c}^{p(\eta)} dp = \int_{\eta=0}^{\eta=\eta} -\frac{\rho\nu^2}{a^2} \left[F_{\eta\eta} + F F_\eta + \alpha \left(F + \eta F_\eta \right) \right], \tag{45}$$

the pressure distribution in the transverse direction can be non-dimensionalized and written as

$$\Delta p_t = \frac{p - p_c}{\rho\nu^2 / a_o^2} \frac{a^2}{a_o^2} = -\left(\alpha\eta F + \tfrac{1}{2} F^2 + F_\eta \right) + F_\eta \Big|_{\eta=0}. \tag{46}$$

Since F behaves as a function of η only and $F_{\eta t} = 0$ in the axial direction, substitution of the velocity components from Eq. (14) into the axial momentum Eq. (2) yields the axial pressure gradient:

$$p_x = \frac{\rho\nu^2 x}{a^4} \left[F''' + F F'' + F' \left(2\alpha - F' \right) + \alpha y F'' \right]. \tag{47}$$

In light of Eq. (23), Eq. (47) can be simplified into

$$p_x = \frac{\rho\nu^2 x}{a^4} K. \tag{48}$$

This can be readily integrated and non-dimensionalized to obtain the axial pressure distribution at any transverse position:

$$\Delta p_a = \frac{p - p_o}{\rho\nu^2 a_o^2} \frac{a^4}{a_o^4} = \frac{K}{2} \frac{x^2}{a_o^2}. \tag{49}$$

Additionally, the shear stress due to flow past the porous surface can be determined. Substituting the velocity components from Eq. (14) into the shear stress equation and non-dimensionalizing yields

$$\Delta\tau_w = \frac{\tau_w}{\rho\nu^2 / a_o^2} \frac{a^3}{a_o^3} = \frac{x}{a_o} \left(F'' \right)_{\eta=1}. \tag{50}$$

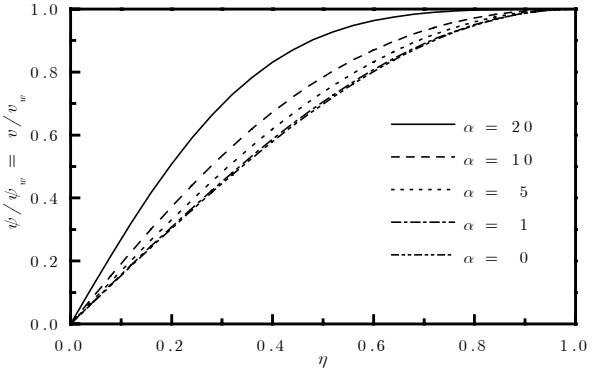

Fig. 2. Stream function and transverse velocity component (*R* = 5).

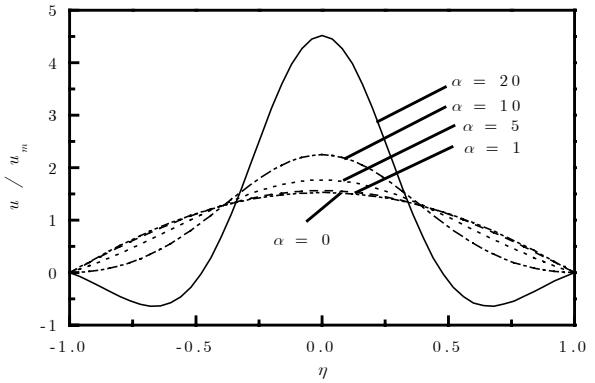

Fig. 3. Axial velocity profiles over range of expansion ratios (*R* = 5).

V. Results

To further expound the results of the presented flow, a variety of values for the expansion ratio α are calculated for the example case scenario of $R = 5$. The stream function for flow under the given parameters is illustrated in Fig. 2. Note that from a comparison of Eq. (42) and (44), the relationships for the normalized stream function and transverse velocities are identical for the entire channel height $0 \le \eta \le 1$. Thus, Fig. 2 also serves to display the transverse velocity distribution. The axial velocity profiles for a range of expansion ratio values are depicted in Fig. 3. As the expansion ratio increases, the axial velocity in the center of the channel also increases. However, at higher values of α, as can be observed at $\alpha = 20$, the velocity near the half range point of the channel height demonstrates reverse flow at lower values of the cross-flow Reynolds number R.

The streamlines for the cases of $\alpha = 0$ and $\alpha = 20$ are illustrated in Figs. 4a and 4b, respectively. For the $\alpha = 20$ plot, the streamlines enter at a steeper angle than the stationary wall case since the former possesses regressing walls which serve to increase the transverse velocity near the walls. We also witness in Fig. 4b that the streamlines rebound rapidly from their nearly co-axial approach. This may ascribed to the regressing walls which act to widen the channel and alleviate the minor throttling effect that would occur for situations experiencing high injection rates relative to the expansion rate.

The transverse pressure distribution computed from Eq. (46) is illustrated in Fig. 5. Note that the pressure drop away from the walls increases as the expansion ratio increases. This may be directly attributed the increased widening of the channel which allows for less restricted flow and, thus, the increased pressure drop. Figure 6 illustrates the axial pressure distribution. Here, the pressure drop decreases with increasing α. Such trends are in agreement with observations made by Weissberg.[24] Figure 7 demonstrates the calculated results of the shear stress at the walls. Clearly, the shear stress increases as the flow travels further down the channel. We also witness a rise in the shear stress as the expansion ratio decreases. For large expansion ratios, the negative axial velocities near the wall are responsible for reversing the shearing stress direction.

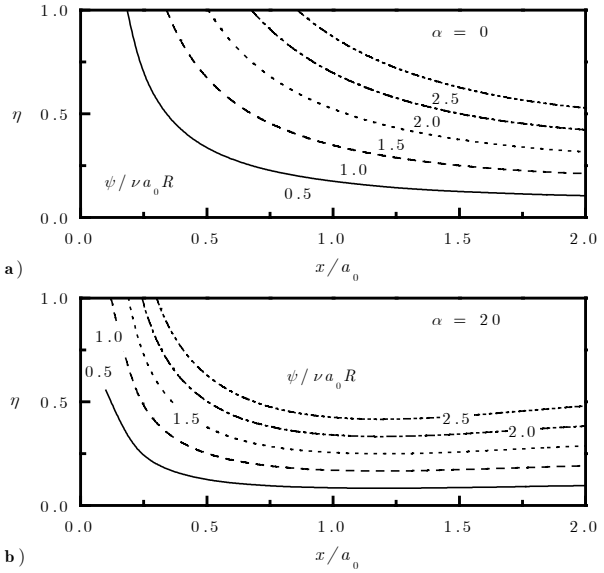

Fig. 4. Streamline patterns for a) $\alpha = 0$ and b) $\alpha = 20$ (R = 5).

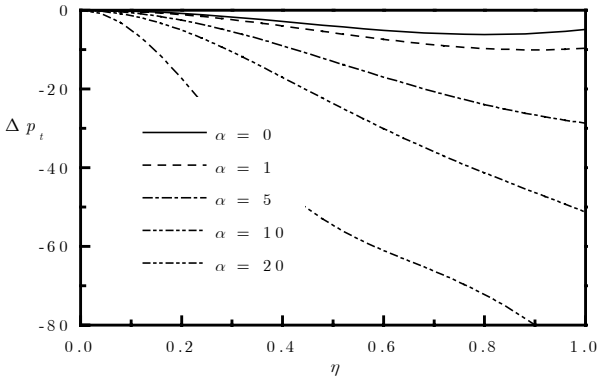

Fig. 5. Normalized transverse pressure distribution over a range of wall expansion ratios (R = 5).

VI. Conclusions

The current analysis presents a procedure that establishes an exact similarity solution of the Navier-Stokes equations in semi-infinite rectangular channels with porous and uniformly expanding walls. It is found that in rectangular chambers and ducts where wall regression and injection occur simultaneously, the streamlines, pressure distributions, and shear stresses are time and space dependent. They can be characterized by two dimensionless parameters: the expansion ratio of the walls α and the cross-flow Reynolds number R. A shooting method, coupled with a Runge-Kutta integration scheme, were utilized to numerically solve the fourth order differential

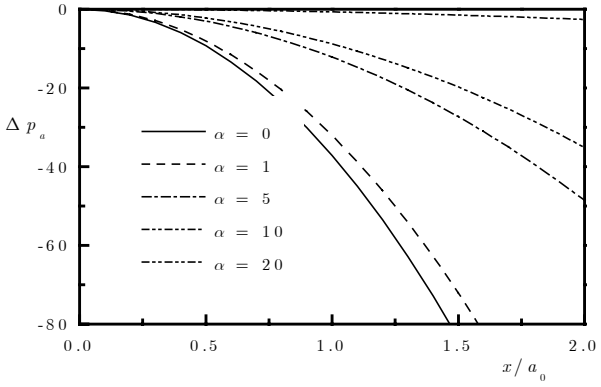

Fig. 6. Normalized axial pressure distribution over a range of wall expansion ratios (R = 5).

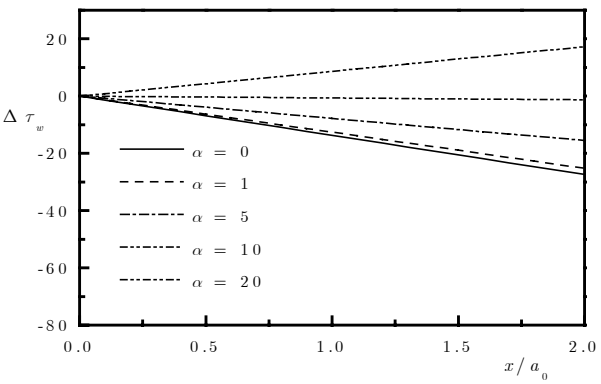

Fig. 7. Wall shearing stress distribution over a range of wall expansion ratios (R = 5).

equation. The results helped explain the flow-field character.

References

[1]Berman, A. S., "Laminar Flow in Channels with Porous Walls," *Journal of Applied Physics,* Vol. 24, No. 9, 1953, pp. 1232-1235.

[2]Sellars, J. R., "Laminar Flow in Channels with Porous Walls at High Suction Reynolds Numbers," *Journal of Applied Physics,* Vol. 26, No. 4, 1955, pp. 489-490.

[3]Terrill, R. M., "Laminar Flow in a Uniformly Porous Channel," *The Aeronautical Quarterly,* Vol. 15, 1964, pp. 299-310.

[4]Proudman, I., "An Example of Steady Laminar Flow at Large Reynolds Number," *Journal of Fluid Mechanics,* Vol. 9, No. 4, 1960, pp. 593-612.

[5]Morduchow, M., "On Laminar Flow through a Channel or Tube with Injection: Application of Method of Averages," *Quarterly Journal of Applied Mathematics,* Vol. 14, No. 4, 1957, pp. 361-368.

[6]White, F. M., Jr., Barfield, B. F., and Goglia, M. J., "Laminar Flow in a Uniformly Porous Channel," *Transactions of the American Society of Mechanical Engineers: Journal of Applied Mechanics, Series E,* Vol. 25, 1958, pp. 613-617.

[7]Taylor, G. I., "Fluid Flow in Regions Bounded by Porous Surfaces," *Proceedings of the Royal Society, London, Series A,* Vol. 234, No. 1199, 1956, pp. 456-475.

[8]Yuan, S. W., "Further Investigation of Laminar Flow in Channels with Porous Walls," *Journal of Applied Physics,* Vol. 27, No. 3, 1956, pp. 267-269.

[9]Terrill, R. M., "Laminar Flow in a Uniformly Porous Channel with Large Injection," *The Aeronautical Quarterly,* Vol. 16, 1965, pp. 323-332.

[10]Terrill, R. M., and Shrestha, G. M., "Laminar Flow Through Parallel and Uniformly Porous Walls of Different Permeability," *Journal of Applied Mathematics and Physics (ZAMP),* Vol. 16, 1965, pp. 470-482.

[11]Shrestha, G. M., and Terrill, R. M., "Laminar Flow with Large Injection Through Parallel and Uniformly Porous Walls of Different Permeability," *Quarterly Journal of Mechanics and Applied Mathematics,* Vol. 21, No. 4, 1968, pp. 413-432.

[12]Cox, S. M., "Two-dimensional Flow of a Viscous Fluid in a Channel with Porous Walls," *Journal of Fluid Mechanics,* Vol. 227, 1991, pp. 1-33.

[13]Brady, J. F., and Acrivos, A., "Steady Flow in a Channel or Tube with an Accelerating Surface Velocity. An Exact Solution to the Navier-Stokes Equations with Reverse Flow," *Journal of Fluid Mechanics,* Vol. 112, 1981, pp. 127-150.

[14]Watson, E. B. B., Banks, W. H. H., Zaturska, M. B., and Drazin, P. G., "On Transition to Chaos in Two-dimensional Channel Flow Symmetrically Driven by Accelerating Walls," *Journal of Fluid Mechanics,* Vol. 212, 1990, pp. 451-485.

[15]Watson, P., Banks, W. H. H., Zaturska, M. B., and Drazin, P. G., "Laminar Channel Flow Driven by Accelerating Walls," *European Journal of Applied Mathematics,* Vol. 2, 1991, pp. 359-385.

[16]Varapaev, V. N., and Yagodkin, V. I., "Flow Stability in a Channel with Porous Walls," *Fluid Dynamics (Izvestiya Akademii Nauk SSSR, Meckanika Zhidkosti i Gaza),* Vol. 4, No. 5, 1969, pp. 91-95.

[17]Raithby, G. D., and Knudsen, D. C., "Hydrodynamic Development in a Duct with Suction and Blowing," *Transactions of the American Society of Mechanical Engineers: Journal of Applied Mechanics, Series E,* Vol. 41, 1974, pp. 896-902.

[18]Sviridenkov, A. A., and Yagodkin, V. I., "Flow in the Initial Sections of Channels with Permeable Walls," *Fluid Dynamics (Izvestiya Akademii Nauk SSSR, Meckanika Zhidkosti i Gaza),* Vol. 11, No. 5, 1976, pp. 689-693.

[19]Ma, Y., Van Moorhem, W. K., and Shorthill, R. W., "Innovative Method of Investigating the Role of Turbulence in the Velocity Coupling Phenomenon," *Journal of Vibration and Acoustics-Transactions of the ASME,* Vol. 112, No. 4, 1990, pp. 550-555.

[20]Ma, Y., Van Moorhem, W. K., and Shorthill, R. W., "Experimental Investigation of Velocity Coupling in Combustion Instability," *Journal of Propulsion and Power,* Vol. 7, No. 5, 1991, pp. 692-699.

[21]Barron, J., Majdalani, J., and Van Moorhem, W. K., "A Novel Investigation of the Oscillatory Field over a Transpiring Surface," AIAA Paper 98-2694, June 1998.

[22]Goto, M., and Uchida, S., "Unsteady Flows in a Semi-infinite Expanding Pipe with Injection Through Wall," *Transactions of the Japan Society for Aeronautical and Space Sciences,* Vol. 33, No. 9, 1990, pp. 14-27.

[23]Uchida, S., and Aoki, H., "Unsteady Flows in a Semi-infinite Contracting or Expanding Pipe," *Journal of Fluid Mechanics,* Vol. 82, No. 2, 1977, pp. 371-387.

[24]Weissberg, H. L., "Laminar Flow in the Entrance Region of a Porous Pipe," *The Physics of Fluids,* Vol. 2, No. 5, 1959, pp. 510-516.